Two-photon–induced internal modification of silicon by erbium-doped fiber laser

P. C. Verburg,* G. R. B. E. Römer, and A. J. Huis in 't Veld

University of Twente, Faculty of Engineering Technology, Chair of Applied Laser Technology, P.O. Box 217, 7500 AE Enschede, The Netherlands

*p.c.verburg@utwente.nl

Abstract: Three-dimensional bulk modification of dielectric materials by multiphoton absorption of laser pulses is a well-established technology. The use of multiphoton absorption to machine bulk silicon has been investigated by a number of authors using femtosecond laser sources. However, no modifications confined in bulk silicon, induced by multiphoton absorption, have been reported so far. Based on results from numerical simulations, we employed an erbium-doped fiber laser operating at a relatively long pulse duration of 3.5 nanoseconds and a wavelength of 1549 nm for this process. We found that these laser parameters are suitable to produce modifications at various depths inside crystalline silicon.

OCIS codes: (140.3390) Laser materials processing; (140.3500) Lasers, erbium; (160.6000) Semiconductor materials; (190.4720) Optical nonlinearities of condensed matter.

References and links

1. R. R. Gattass and E. Mazur, "Femtosecond laser micromachining in transparent materials," Nat. Photonics **2**, 219–225 (2008).
2. J. Qiu, K. Miura, and K. Hirao, "Femtosecond laser-induced microfeatures in glasses and their applications," J. Non-Cryst. Solids **354**, 1100–1111 (2008).
3. N. M. Bulgakova, R. Stoian, and A. Rosenfeld, "Laser-induced modification of transparent crystals and glasses," Quantum Electron. **40**, 966 (2010).
4. E. G. Gamaly and A. V. Rode, "Physics of ultra-short laser interaction with matter: From phonon excitation to ultimate transformations," Prog. Quantum Electron. **37**, 215–323 (2013).
5. M. Mirkhalaf, A. K. Dastjerdi, and F. Barthelat, "Overcoming the brittleness of glass through bio-inspiration and micro-architecture," Nat. Commun. **5**, 3166 (2014).
6. S. Juodkazis, K. Nishimura, S. Tanaka, H. Misawa, E. G. Gamaly, B. Luther-Davies, L. Hallo, P. Nicolai, and V. T. Tikhonchuk, "Laser-induced microexplosion confined in the bulk of a sapphire crystal: Evidence of multimegabar pressures," Phys. Rev. Lett. **96**, 166101 (2006).
7. E. N. Glezer and E. Mazur, "Ultrafast-laser driven micro-explosions in transparent materials," Appl. Phys. Lett. **71**, 882–884 (1997).
8. E. G. Gamaly, S. Juodkazis, K. Nishimura, H. Misawa, B. Luther-Davies, L. Hallo, P. Nicolai, and V. T. Tikhonchuk, "Laser-matter interaction in the bulk of a transparent solid: Confined microexplosion and void formation," Phys. Rev. B **73**, 214101 (2006).
9. A. H. Nejadmalayeri, P. R. Herman, J. Burghoff, M. Will, S. Nolte, and A. Tünnermann, "Inscription of optical waveguides in crystalline silicon by mid-infrared femtosecond laser pulses," Opt. Lett. **30**, 964 (2005).
10. V. V. Parsi Sreenivas, M. Bülters, and R. B. Bergmann, "Microsized subsurface modification of mono-crystalline silicon via non-linear absorption," J. Eur. Opt. Soc. Rapid Pub. **7**, 12035 (2012).
11. E. Ohmura, F. Fukuyo, K. Fukumitsu, and H. Morita, "Internal modified-layer formation mechanism into silicon with nanosecond laser," J. Achiev. Mater. Manuf. Eng. **17**, 381 (2006).
12. E. Ohmura, "Temperature rise of silicon due to absorption of permeable pulse laser," in "Heat Transfer - Engineering Applications," , V. S. Vikhrenko, ed. (InTech, 2011), Chap. 2.

#214633 - $15.00 USD Received 23 Jun 2014; revised 14 Aug 2014; accepted 22 Aug 2014; published 3 Sep 2014

13. Y. Izawa, S. Tanaka, H. Kikuchi, Y. Tsurumi, N. Miyanaga, M. Esashi, and M. Fujita, "Debris-free in-air laser dicing for multi-layer MEMS by perforated internal transformation and thermally-induced crack propagation," in "IEEE 21st International Conference on Micro Electro Mechanical Systems," (2008).
14. R. Singh, Y. Audet, Y. Gagnon, Y. Savaria, E. Boulais, and M. Meunier, "A laser-trimmed rail-to-rail precision CMOS operational amplifier," IEEE Trans. Circuits Syst. II, Exp. Briefs **58**, 75–79 (2011).
15. E. Boulais, J. Fantoni, A. Chateauneuf, Y. Savaria, and M. Meunier, "Laser-induced resistance fine tuning of integrated polysilicon thin-film resistors," IEEE Trans. Electron Dev. **58**, 572–575 (2011).
16. L. Rapp, B. Haberl, J. E. Bradby, E. G. Gamaly, J. S. Williams, and A. V. Rode, "Confined micro-explosion induced by ultrashort laser pulse at SiO2/Si interface," Appl. Phys. A: Mater. **114**, 33–43 (2014).
17. V. V. Kononenko, V. V. Konov, and E. M. Dianov, "Delocalization of femtosecond radiation in silicon," Opt. Lett. **37**, 3369 (2012).
18. S. Leyder, D. Grojo, P. Delaporte, W. Marine, M. Sentis, and O. Utéza, "Multiphoton absorption of 1.3 μm wavelength femtosecond laser pulses focused inside Si and SiO_2," Proc. SPIE **8770**, 877004 (2013).
19. P. C. Verburg, G. R. B. E. Römer, G. H. M. Knippels, J. Betz, and A. J. Huis in 't Veld, "Experimental validation of model for pulsed-laser–induced subsurface modifications in Si," in "Proceedings of the 13th International Symposium on Laser Precision Microfabrication, June 12-15 2012, Washington DC, USA," (2012).
20. P. C. Verburg, G. R. B. E. Römer, and A. J. Huis in 't Veld, "Two-temperature model for pulsed-laser–induced subsurface modifications in Si," Appl. Phys. A: Mater. **114**, 1135–1143 (2014).
21. G. E. Jellison, Jr. and D. H. Lowndes, "Optical absorption coefficient of silicon at 1.152 μm at elevated temperatures," Appl. Phys. Lett. **41**, 594–596 (1982).
22. E. V. Zavedeev, V. V. Kononenko, V. M. Gololobov, and V. I. Konov, "Modeling the effect of fs light delocalization in Si bulk," Laser Phys. Lett. **11**, 036002 (2014).
23. A. Singh, "Free charge carrier induced refractive index modulation of crystalline silicon," in "IEEE International Conference on Group IV Photonics," (2010), pp. 102–104.
24. M. A. Green, "Self-consistent optical parameters of intrinsic silicon at 300K including temperature coefficients," Sol. Energy Mater. Sol. Cells **92**, 1305–1310 (2008).
25. A. D. Bristow, N. Rotenberg, and H. M. van Driel, "Two-photon absorption and Kerr coefficients of silicon for 850-2200 nm," Appl. Phys. Lett. **90**, 191104 (2007).
26. H. M. van Driel, "Kinetics of high-density plasmas generated in Si by 1.06- and 0.53-μm picosecond laser pulses," Phys. Rev. B **35**, 8166–8176 (1987).
27. A. L. Smirl, I. W. Boyd, T. F. Boggess, S. C. Moss, and H. M. van Driel, "Structural changes produced in silicon by intense 1-μm ps pulses," J. Appl. Phys. **60**, 1169–1182 (1986).
28. A. Lietoila and J. F. Gibbons, "Computer modeling of the temperature rise and carrier concentration induced in silicon by nanosecond laser pulses," J. Appl. Phys. **53**, 3207–3213 (1982).
29. J. Chen, D. Tzou, and J. Beraun, "Numerical investigation of ultrashort laser damage in semiconductors," Int. J. Heat Mass Transf. **48**, 501–509 (2005).
30. M. W. Chase, "NIST-JANAF thermochemical tables," J. Phys. Chem. Ref. Data Monograph 9 (1998).
31. M. J. Nasse and J. C. Woehl, "Realistic modeling of the illumination point spread function in confocal scanning optical microscopy," J. Opt. Soc. Am. A **27**, 295–302 (2010).
32. N. G. Nilsson, "Band-to-band Auger recombination in silicon and germanium," Phys. Scripta **8**, 165 (1973).
33. C. J. Glassbrenner and G. A. Slack, "Thermal conductivity of silicon and germanium from 3°K to the melting point," Phys. Rev. **134**, A1058–A1069 (1964).
34. F. Berz, R. W. Cooper, and S. Fagg, "Recombination in the end regions of pin diodes," Solid State Electron. **22**, 293–301 (1979).
35. T. Wang, N. Venkatram, J. Gosciniak, Y. Cui, G. Qian, W. Ji, and D. T. H. Tan, "Multi-photon absorption and third-order nonlinearity in silicon at mid-infrared wavelengths," Opt. Express **21**, 32192–32198 (2013).
36. M. Kumagai, T. Sakamoto, and E. Ohmura, "Laser processing of doped silicon wafer by the stealth dicing," in "International Symposium on Semiconductor Manufacturing 2007," (2007).
37. J. E. Peters, P. D. Ownby, C. R. Poznich, J. C. Richter, and D. W. Thomas, "Infrared absorption of Czochralski germanium and silicon," Proc. SPIE **4452**, 17–24 (2001).
38. G. Zhu, J. van Howe, M. Durst, W. Zipfel, and C. Xu, "Simultaneous spatial and temporal focusing of femtosecond pulses," Opt. Express **13**, 2153–2159 (2005).
39. D. Oron, E. Tal, and Y. Silberberg, "Scanningless depth-resolved microscopy," Opt. Express **13**, 1468–1476 (2005).

1. Introduction

Within the research on the interaction of laser beams with materials, the three-dimensional machining of transparent dielectric materials has received considerable attention [1–8]. This process is also referred to as the production of subsurface, bulk or internal modifications. Many optical applications of this method are based on laser-induced refractive index changes, which

#214633 - $15.00 USD Received 23 Jun 2014; revised 14 Aug 2014; accepted 22 Aug 2014; published 3 Sep 2014

can be both positive and negative compared with the unmodified material [1]. Optical applications include three-dimensional data-storage and the production of waveguides, gratings, lenses, attenuators and crystals [2–4]. Moreover, it has been shown that laser-induced subsurface modifications can be applied for the strengthening of glass [5]. Finally, confined laser-material interaction may be used to generate pressures in the TPa range, to study the behavior of matter under extreme conditions [6–8].

In addition to dielectrics, the formation of laser-induced subsurface modifications is of interest for the machining of silicon. Similar to dielectric materials, internal modifications could be applied for the inscription of optical devices [9, 10]. As silicon is the material of choice for the production of integrated circuits, this may allow electronics and optical components to be integrated on a single chip [9].

Another application of subsurface modifications in silicon is wafer dicing [11, 12]. Wafer dicing by means of laser-induced subsurface modifications is a process that consists of two steps (see Fig. 1). First, short laser pulses are focused inside the wafer. Each laser pulse results in the production of a subsurface modification. Secondly, after laser processing, an external force is exerted on the wafer. As a result, the wafer fractures along the planes containing the subsurface modifications, thereby separating the wafer into dies. This wafer dicing method is especially beneficial for the separation of sensitive devices such as microelectromechanical systems, as it is dry and debris-free [13]. For multi-layer microelectromechanical systems consisting of both silicon and glass, a combination of a nanosecond laser with a wavelength of 1064 nm to modify the silicon and a 800 nm femtosecond laser to modify the glass has been proposed [13].

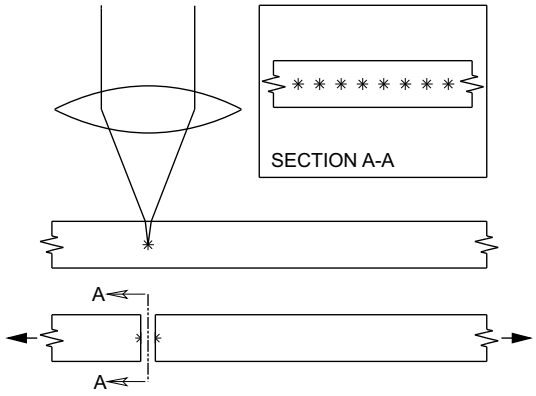

Fig. 1. Schematic overview of the process to fracture silicon wafers, using pulsed-laser–induced subsurface modifications. First, laser-induced modifications are created below the surface of the wafer (top). The modifications are indicated by asterisks $(*)$. Next, an external force is exerted on the wafer, which causes the wafer to separate along the planes containing laser modifications (bottom).

Besides wafer dicing, laser modifications have been employed to precisely control the resistivity of thin polycrystalline silicon films buried under layers of dielectric material [14, 15], for use in precision analog devices. The change in resistivity is expected to be due to localized crystallization at grain boundaries, induced by heating the material to a temperature below the melting point [15]. The laser-induced subsurface modification technology could allow for such resistivity changes to be produced, even when the volume that is to be modified is located below silicon layers.

Finally, recent results obtained using laser pulses focused on a silicon-silicon oxide interface have shown that novel phases could possibly be generated [16]. The subsurface modification

#214633 - $15.00 USD Received 23 Jun 2014; revised 14 Aug 2014; accepted 22 Aug 2014; published 3 Sep 2014

method might be capable of producing such phases in three-dimensional patterns, without the need for a sandwich structure of two materials.

For the formation of subsurface modifications inside dielectrics, multiphoton absorption is generally applied [1]. Since multiphoton absorption depends on the square or higher powers of the intensity of the light, it allows for better confinement of the absorption of laser energy than can be achieved by merely focusing the beam. Recently, several authors studied the formation of subsurface modification in silicon using two-photon and three-photon absorption [9, 10, 17, 18], in addition to studies that employed a photon energy near the band-gap of silicon [12, 13, 19]. The experimental conditions that were applied during these studies are listed in table 1. For each set of experimental conditions, the number of photons involved in the interband absorption of laser energy and the outcome of the experiments are indicated.

Table 1. Overview of processing conditions that were previously investigated for the formation of laser-induced subsurface modifications in crystalline silicon. λ: Wavelength, # photons: the number of photons involved in the interband absorption of laser energy, NA: numerical aperture.

λ (# photons)	Pulse duration	Pulse energy	NA	Result	Ref.
1030 nm (1–2)	6.6 ps	<2.1 µJ	0.7	No subsurface modifications	[19]
1064 nm (1–2)	150 ns	4 µJ	—	Subsurface modifications	[12]
1064 nm (1–2)	> 8 ns	0.5–14 µJ	0.7	Subsurface modifications	[19]
1064 nm (1–2)	10 ns	0.5–12 µJ	0.7	Subsurface modifications	[13]
1200 nm (2)	250 fs	<90 µJ	0.2	No subsurface modifications	[17]
1300 nm (2)	100 fs	<730 nJ	0.3	No subsurface modifications	[18]
1550 nm (2)	800 fs	50 µJ	1.25	Surface and subsurface damage	[10]
2400 nm (3)	70 fs	1.7 µJ	0.5	Modifications below oxide	[9]

When considering the studies referred to in table 1, subsurface modifications were only successfully produced using a wavelength of 1064 nm, where single-photon absorption still has a significant contribution to the total absorption of laser energy. During two studies based on two-photon absorption, no modifications were found [17, 18], even when applying multiple pulses with energies up to 90 µJ [17]. One study using three-photon absorption resulted in modifications at a silicon-silicon oxide interface [9]. However, no modifications could be created deeper inside silicon, when placing the focus inside the silicon layer [9]. Finally, evidence of subsurface damage was found in a recent study using an oil immersion objective with a numerical aperture of 1.25 [10]. However, despite the high numerical aperture, surface damage was reported [10]. One property that all previous multiphoton experiments have in common is that femtosecond lasers were employed.

The success of the 1064 nm process, corresponding to a photon energy near the band-gap of silicon, is based on a thermal runaway [12, 20]. Because the linear absorption coefficient of silicon strongly increases with temperature for photon energies near the band-gap [21], an initial temperature rise results in a higher absorptivity, creating an even faster increase in temperature. Hence, a positive feedback can be established. However, since single-photon interband absorption will occur regardless of the level of the light intensity, the selectivity of the process is limited and higher energy losses will occur when focusing deeper below the surface.

The aim of the current study is to develop a multiphoton subsurface modification method that is suitable for crystalline silicon.

#214633 - $15.00 USD Received 23 Jun 2014; revised 14 Aug 2014; accepted 22 Aug 2014; published 3 Sep 2014

2. Laser energy absorption in bulk silicon

For the formation of laser-induced modifications inside silicon to succeed, sufficient energy should be transferred to the silicon in a small subsurface volume, regardless of the damage mechanism. The following requirements can be established to accomplish this goal: (1) the laser pulse should be sufficiently short to prevent the absorbed energy from being conducted away from the location of the focal spot, (2) the laser pulse should contain enough energy to induce a modification and (3) the laser energy should be efficiently absorbed in and near the focal spot.

The question is which of these requirements has not been fulfilled during previous studies employing femtosecond pulses. Heat conduction and carrier diffusion are negligible during femtosecond pulses such that requirement (1) is fulfilled. Requirement (2) is also unlikely to be violated. For a pulse energy of 90 µJ, no subsurface damage could be found [17], even though this energy value is two orders of magnitude beyond the required energy to form a subsurface modification [12, 13, 19].

Based on the above, the only plausible explanation for previous femtosecond experiments failing to form modifications would be that requirement (3) is not satisfied. The physical phenomena that may cause delocalization of the absorption of laser energy are listed below.

1. The instantaneous power of the laser beam exceeding the threshold for self-focusing [8]. Self-focusing is related to the dependence of the refractive index on the laser intensity, which is known as the Kerr effect.

2. Too strong multiphoton absorption before the beam reaches the focal plane, resulting in:

   (a) A large part of the laser energy not reaching the volume that should be modified. The same conditions as used for the experiments in Ref. [17] have been evaluated by numerical simulations [22]. The simulations showed that less than one percent of the laser energy reached the focal plane for a 250 fs pulse with a pulse energy of 100 µJ and a wavelength of 1200 nm.

   (b) Plasma-induced beam defocusing due to transverse gradients in the refractive index. The refractive index of silicon decreases with increasing carrier density [23]. Evidence for plasma-defocusing when focusing femtosecond pulses inside silicon has been found by infrared interferometry [17].

The critical power for self-focusing is given by [8]

$$P_{\text{critical}} = \frac{\lambda^2}{2\pi n_0 n_2},$$

in which n_0 are n_2 are the linear and nonlinear part of the refractive index: $n = n_0 + n_2 I$, where I is the laser intensity. For the wavelength range of 1200-1550 nm, $n_0 \approx 3.5$ [24] and $n_2 \approx 4.5 \times 10^{-14}\,\text{cm}^2/\text{W}$ [25]. This results in a critical power of approximately 24 kW for a wavelength of 1549 nm. When assuming the temporal power profile of the laser pulse to be Gaussian, with the pulse duration defined as the full width at half maximum, the critical pulse energy for the 3.5 ns/1549 ns process that is considered in this work is ≈ 90 µJ. This energy is well above the pulse energies that were applied during our experiments (up to 4 µJ, see Sec. 7). For the conditions used during the femtosecond experiments listed in table 1, the critical pulse energies are in the order of tens of nanojoules, implying that self-focusing due to the Kerr effect is an important issue.

#214633 - $15.00 USD Received 23 Jun 2014; revised 14 Aug 2014; accepted 22 Aug 2014; published 3 Sep 2014

3. Laser intensity distribution and modification mechanisms

In this work, a modification is defined as any permanent change to the material structure, induced by the laser process. For the prediction of surface damage of crystalline silicon induced by laser pulses, melting has been reported to be an accurate indicator [26–29]. Due to the fast cooling that occurs after the laser pulse, the molten silicon does not fully return to its original low-defect monocrystalline state.

To assess whether melting and fast resolidification is also a plausible damage mechanism during the subsurface modification process, the density of absorbed laser energy has to be considered. The amount of energy that is required to heat silicon from room temperature to the melting point and to overcome the latent heat of fusion is 86 kJ/mol [30]. Based on a density of 2.33 gm/cm^3 and a molar mass of 28.09 g/mol, this corresponds to an energy density of 7.1×10^3 J/cm^3.

To approximate the volume in which the laser energy is absorbed, the intensity distribution inside silicon has been computed using the PSF Lab software [31], based on a non-absorbing material with a homogeneous refractive index. This software takes non-paraxial propagation into account, including the coverslip correction of the microscope objective. The conditions were matched to the laser source and optical system presented in Sec. 5.

A cross-section of the axisymmetric intensity distribution is shown in Fig. 2. Since the focus location matches the coverslip correction, no spherical aberrations are present. However, some diffraction that is caused by the aperture of the objective blocking a part of the Gaussian laser beam is visible. The focal spot has a $1/e^2$ diameter of 2.4 µm. Similarly, the focal volume is defined as the volume in which the laser intensity exceeds the peak intensity multiplied by $1/e^2$. The corresponding contour is indicated by a black line in Fig. 2, which represents a volume of 176 µm^3.

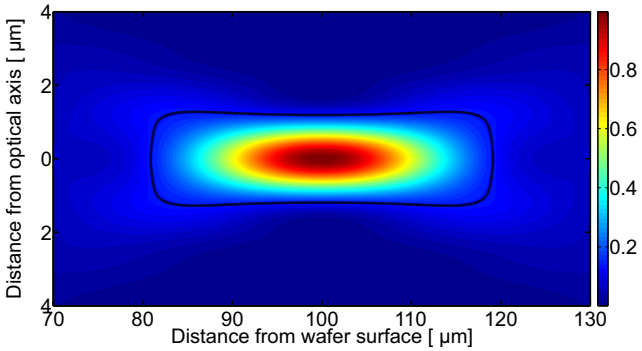

Fig. 2. Cross-section of the axisymmetric laser intensity distribution inside silicon [arbitrary units]. The black line indicates the contour where the intensity has dropped to a factor $1/e^2$ of the peak intensity. The laser beam has a Gaussian spatial distribution before entering the objective. The $1/e^2$ radius of the beam fills 80 percent of the aperture of the objective. The beam is focused 100 µm below the surface, which matches the coverslip correction of the microscope objective. Wavelength: 1549 nm, beam quality: $M^2 = 1.1$, numerical aperture: 0.7, refractive index: 3.5. Note the difference in scale between the horizontal and vertical axis, the focal volume is strongly elongated along the optical axis.

The volume that is heated by the laser may be larger than the focal volume, due to the diffusion of carriers, electronic heat conduction and lattice heat conduction. Since numerical simulations showed that diffusion effects have little effect during subsurface processing of silicon on a short nanosecond timescale [20], the extension of the laser-heated volume by diffusion

#214633 - $15.00 USD Received 23 Jun 2014; revised 14 Aug 2014; accepted 22 Aug 2014; published 3 Sep 2014

has been neglected. A study of nanosecond surface heating of silicon also reported limited effects of carrier diffusion and electronic heat conduction [28]. An important contributing factor to these results is that the lifetime of the carriers is far shorter than the pulse duration due to Auger recombination. Typical carrier densities for laser processing of silicon are in the range of 10^{19} to 10^{21} cm^{-3} [26]. At a density of 10^{20} cm^{-3}, a high-temperature Auger recombination coefficient of 4×10^{-30} cm^6/s [32] results in a lifetime of 25 ps. Moreover, the total conductivity of silicon [33] and the mobility of the electrons and holes [34] decrease with temperature. Further mobility reductions occur due to electron-hole scattering at high carrier densities [34].

A complicating factor when establishing the volume, in which the laser energy is absorbed, is that it strongly depends on the processing conditions. For a fixed pulse duration, higher pulse energies result in effective two-photon absorption at larger distances from the focal plane, as the intensities throughout the beam path are higher. The experimentally observed modification lengths (see Sec. 7) give an indication regarding the extent of the laser-heated volume. A pulse energy around 3 µJ was required (see Fig. 9), to create a subsurface modification with the same length as the focal volume defined above. Taking a surface reflectivity of 30 percent into account, this yields an energy density of $\approx 1.2 \times 10^4$ J/cm^3 in the focal volume, which exceeds the required energy density of 7.1×10^3 J/cm^3 for melting of silicon.

Based on the above, melting and fast resolidification is expected to be an important damage mechanism for the subsurface modification process. However, other mechanisms cannot be ruled out. Due to the evidence that very high pressures can be generated when focusing a laser beam inside solid material [6–8], pressure-induced phase transitions may occur.

4. Selection of processing conditions

To prevent linear absorption, a wavelength above ≈ 1.2 µm is required to produce multiphoton-induced subsurface modifications in silicon. For practical reasons, a wavelength around 1550 nm in the optical communications C-band was selected, based on the availability of laser sources and optical components at this wavelength. The corresponding photon energy of 0.8 eV is well below the band-gap of silicon, such that the linear interband absorption is negligible [25]. However, it is sufficiently high to enable two-photon absorption at high light intensities [25]. Moreover, wavelengths around 1550 nm result in strong multiphoton absorption compared to the influence of the Kerr effect [35].

To select suitable processing conditions for the two-photon process, numerical simulations were performed using a model that we published previously [20]. The simulations were carried out for an optical system that matches the experimental set-up presented in Sec. 5. The required pulse energy was determined by the amount of energy that is needed to melt a volume of silicon, in the vicinity of the focus of the beam (see Sec. 3). For a fixed wavelength, pulse energy and optical system, the pulse duration can be optimized to obtain the required intensities throughout the beam path. Based on the simulation results, a laser source with a pulse duration of 3.5 ns was selected to obtain efficient two-photon and subsequent free carrier absorption near the focus of the beam, while preventing self-focusing due to the Kerr effect.

5. Material and laser machining set-up

For the experiments, 160-µm thick p-type monocrystalline <100> silicon wafers with a resistivity of 10.3 ohm-cm were used. Previous research has shown that this resistivity is sufficiently high to preclude appreciable absorption of laser energy by the equilibrium carrier concentration [36].

A schematic overview of the experimental setup is shown in Fig. 3. The laser source that was used is an erbium-doped fiber laser, based on a master oscillator power amplifier architecture (MWTechnologies MOPA-LF-1550). This laser was configured for operation at low repetition

#214633 - $15.00 USD Received 23 Jun 2014; revised 14 Aug 2014; accepted 22 Aug 2014; published 3 Sep 2014

rates, without excessive amplified spontaneous emission between subsequent pulses. The laser source provides pulses with a fixed full width at half maximum duration of 3.5 nanoseconds at a wavelength of 1549 nm. The spatial beam profile is Gaussian with an M^2 below 1.1. A maximum energy per pulse of 20 µJ was available. After exiting the collimator, the laser beam was polarized by a polarizing beamsplitter and was subsequently attenuated by a half-lambda waveplate and another polarizing beamsplitter, to obtain the desired pulse energy. Next, the laser beam diameter was expanded such that the $1/e^2$ beam diameter fills 80 percent of the back aperture of the microscope objective.

The microscope objective (Leica Microsystems 11 101 666), that was used to focus the laser pulses inside the silicon samples, has a numerical aperture of 0.7, a focal length of 3.27 mm and a coverslip correction for 100 µm of silicon. If the focus depth inside silicon is matched to the coverslip correction, the focal spot has a $1/e^2$ diameter of 2.4 µm (see Sec. 3). When placing modifications near the surface of the silicon wafer or creating surface marks, the objective was protected by a 250-µm thick quartz window to prevent damage to the objective by ablated material. As this window induces negative spherical aberrations because of a mismatch in coverslip correction, no window was used during the quantitative measurements presented in Sec. 7.2.

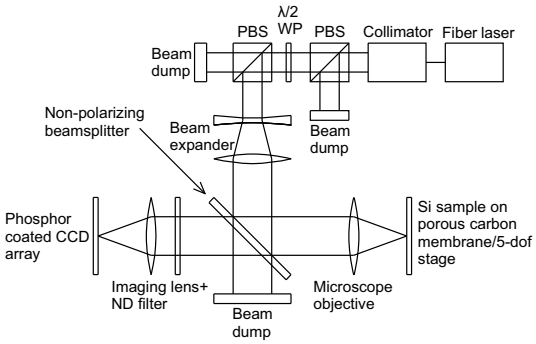

Fig. 3. Schematic overview of the experimental setup. WP: Waveplate, PBS: polarizing beamsplitter, ND: neutral density, dof: degrees of freedom, CCD: charge-coupled device.

To calibrate the focus position and to align the samples with respect to the objective, a non-polarizing beamsplitter was employed that transmits approximately one percent of the laser light reflected from the silicon surface. An additional lens was used to image the reflected laser spot on an image sensor with an anti-Stokes phosphor coating and a filter to block visible light (Applied Scintillation Technologies, Digital CamIR 1550). The phosphor coating upconverts the energy of the photons, such that they can be visualized by a silicon charge-coupled device. The energy of the laser pulses was measured using a Germanium photodiode and a neutral density filter. Calibration measurements were performed behind the microscope objective to obtain the actual on-sample pulse energy. A narrow laser beam was employed for these measurements to prevent errors due to the dependence of the sensor sensitivity on the angle of incidence. The silicon samples were kept in place by a low vacuum behind a porous carbon membrane with better than 500 nm flatness, attached to an automated 5 degrees of freedom stage. Accurate positioning of the sample is important when producing subsurface modifications in silicon. Due to the high refractive index of silicon, errors in the position of the sample along the optical axis are amplified by a factor 3.5, when considering the position of the focus inside the sample.

After calibration of the focus position, the samples were translated to position the focal spot of the microscope objective inside the samples. The repetition rate of the laser was fixed at 100 Hz. By varying the speed of the stage, the spacing between the subsurface modifications

#214633 - $15.00 USD Received 23 Jun 2014; revised 14 Aug 2014; accepted 22 Aug 2014; published 3 Sep 2014

was adjusted. When modifications were produced at different focus depths, the deepest modifications were created first, to prevent the laser beam from being affected by previously created modifications.

6. Detection and analysis tools

Compared with surface features, the analysis of subsurface modifications in silicon is challenging, as they are surrounded by unmodified material. In this section, methods to detect permanent modifications of the material inside bulk silicon are proposed, based on changes to their optical properties and the structural morphology of cleavage planes.

To identify the presence of subsurface damage in a non-destructive manner, infrared transmission microscopy was applied. For this purpose, an optical microscope (Leica DMRM) equipped with a transmitted infrared light source consisting of a halogen light bulb and a long-pass filter was employed. A silicon CMOS camera was used to observe the transmitted light. Consequently, a narrow wavelength range around one micrometer, where the substrate becomes transparent while the camera still provides some sensitivity, was imaged. Infrared microscopy was found to be capable of detecting the presence of subsurface modifications, making it suitable to measure modification thresholds. For the modifications to be visible, the optical axis of the microscope had to be perpendicular to the surface of the wafer.

Simultaneously with the analysis of the samples using infrared light, both bright and dark field illumination with reflected visible light were employed to check for any signs of surface damage. It has been reported that optical microscopy is a suitable method for the detection of inadvertent surface damage while attempting to produce subsurface modifications, even when this damage is not yet obvious from profile measurements [10]. We also found that inadvertent surface damage is readily observable by optical microscopy. Once a modification is on the surface of the wafer, the reflectivity of the surface changes and the amount of scattered light is increased.

While infrared microscopy is suitable to detect whether subsurface modifications are present, it does not provide detailed information about the geometry of the modifications. To obtain more detailed data, destructive analysis methods were applied. For this purpose, multiple layers of subsurface modifications were produced along tracks inside silicon wafers (see Fig. 4). This allows for the silicon samples to be fractured along the plane containing the laser-induced modifications, when a mechanical force is exerted on the sample. Consequently, the issue of localizing the micrometer-sized modifications is prevented, as the modifications themselves determine how the sample will break. To allow separate modifications to be analyzed, such modifications were created in the vicinity of dense modified layers, as shown in Fig. 4.

After fracturing the samples, the exposed surfaces were analyzed using a laser scanning confocal microscope (Keyence VK-9710) and a scanning electron microscope (Jeol JSM-6400).

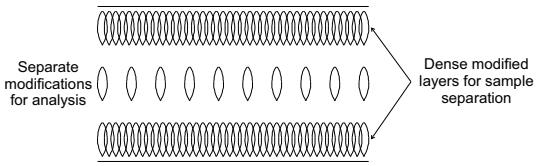

Fig. 4. Schematic drawing of a cross-section of a silicon wafer, showing a pattern of subsurface modifications. The propagation direction of the laser beam is from top to bottom. Dense layers with a close spacing between the modifications are intended to fracture the wafer along the plane containing the laser-induced modifications. Separate modifications are required to study the properties of single-pulse modifications, without the laser beam interacting with previously modified material.

#214633 - $15.00 USD Received 23 Jun 2014; revised 14 Aug 2014; accepted 22 Aug 2014; published 3 Sep 2014

7. Results

First, the feasibility of creating subsurface modifications in crystalline silicon using a combination of a 1549 nm wavelength and a pulse duration of 3.5 ns was investigated. It was found that subsurface modifications could indeed be produced. Figure 5 shows an example of a track of subsurface modifications between two laser-machined surface grooves. The top and bottom parts of the figure show the images obtained using reflected visible light and transmitted infrared light respectively. In visible light (see Fig. 5 (top)), only the two surface grooves can be identified in addition to debris originating from the material ejected from the grooves. When employing infrared light and placing the focus of the microscope inside the sample (see Fig. 5 (bottom)), both the surface grooves and the subsurface modifications are visible, with the surface grooves being out of focus. This shows that the modifications are located below the surface of the silicon sample.

As the subsurface modifications are visible by infrared microscopy, their optical properties differ from the original almost defect-free monocrystalline material. Since subsurface melting of silicon is likely to occur during the modification process (see Sec. 3), resolidification into an amorphous phase, polycrystalline phase or monocrystalline phase with defects may be responsible for the observed contrast in optical microscopy. The contrast may be due to: (1) the material phases generated by the laser process having different optical properties compared with monocrystalline silicon and (2) changes in the optical properties due to internal stresses.

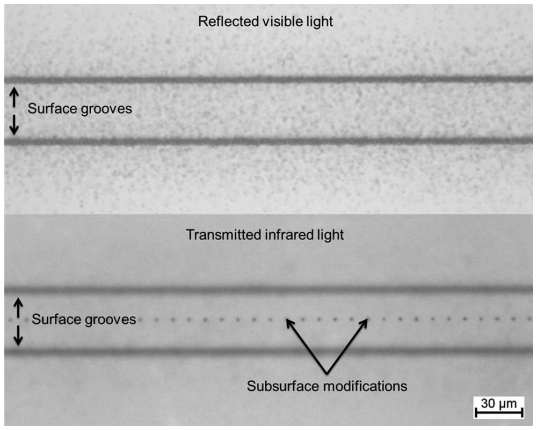

Fig. 5. Brightfield optical microscopy (top) and infrared transmission microscopy (bottom) images of a track of subsurface modifications (top view). Two surface grooves were produced above and below the track. Pulse energy on-sample: 1.3 µJ, focal spot: 70 µm below the surface.

7.1. Closely spaced modifications for wafer dicing

After establishing that modifications could be created, the suitability of these modifications for wafer dicing was investigated. Figure 6 shows a side wall of a die that was separated using subsurface modifications induced by two-photon absorption. Three laser-modified layers were created in this sample by placing the focal spot at different depths inside the silicon sample. The top and bottom layers were located such that no damage to either the front or back surface of the sample could be found before fracturing the sample. The laser pulses, and therefore also the modifications, were spaced 2 µm apart in lateral direction. This spacing was found to be a necessary condition for the fracture plane to reliably follow the plane containing the

#214633 - $15.00 USD Received 23 Jun 2014; revised 14 Aug 2014; accepted 22 Aug 2014; published 3 Sep 2014

laser-induced modifications. Due to the close spacing between the modifications, some interaction with previously laser-modified material will occur during each laser pulse. Therefore, the resulting modifications may differ from single-pulse modifications.

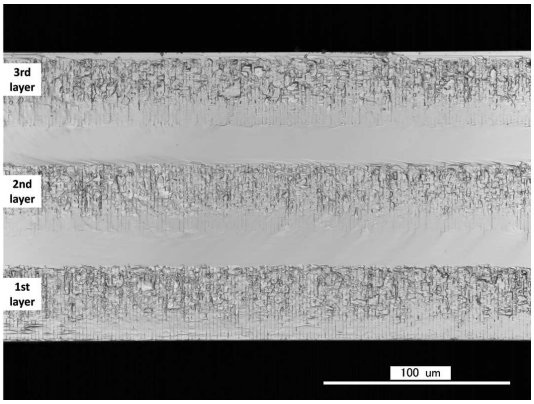

Fig. 6. Laser scanning confocal microscopy image (integrated intensity) of a fracture plane containing pulsed-laser–induced subsurface modifications. Three layers of modifications at different focus depths are visible. The lateral spacing between the laser-induced modifications is 2 µm. Pulse energy on-sample: 1.3 µJ. A 250-µm thick quartz window was used to protect the objective. The laser beam propagation direction is from top to bottom.

To get some insight in the possible damage mechanisms that are responsible for the formation of the subsurface modifications, the modifications shown in Fig. 6 were analyzed in more detail using scanning electron microscopy. Figure 7 shows a detail of the center modified layer of the sample that is presented in Fig. 6. Straight vertical lines can be observed at distances corresponding to the spacing between the laser pulses. Therefore, these features are expected to be located on the optical axis of the laser beam. Along these lines, a number of voids are present. A hypothesis is that the straight vertical lines are related to the location where the material resolidifies last, since melting and resolidification was found to be a plausible damage mechanism (see Sec. 3). Moreover, the voids suggest that elsewhere in the laser-induced modifications an increase in density has occurred, either due to compressive stresses or due to a transformation from the diamond cubic to a denser phase.

7.2. Single-pulse modifications

To quantitatively measure the shapes of subsurface modifications and the required conditions for their formation, single-pulse modifications were analyzed. First, the pulse energy threshold for the production of modifications was determined, for a focus depth of 100 µm below the surface of the silicon sample. For this purpose, similar subsurface modifications as shown in Fig. 5 were produced while varying the pulse energy. By determining the lowest pulse energy for which modifications were visible, the modification threshold was identified. The lower threshold for the on-sample pulse energy was found to be 0.43 µJ, while increasing the pulse energy in steps of 0.07 µJ. For these measurements, the location of the focus and the coverslip correction of the microscope objective have been matched. Moreover, no window was placed between the sample and objective. This ensures that the measurements are not affected by spherical aberrations.

The estimated peak intensity in the focus at the threshold pulse energy, excluding the effect of absorption, is $5.1 \times 10^9 \mathrm{W/cm^2}$. This is an overestimation of the actual value during the laser process, as laser energy will be absorbed before the beam reaches the focal plane. This effect

#214633 - $15.00 USD Received 23 Jun 2014; revised 14 Aug 2014; accepted 22 Aug 2014; published 3 Sep 2014

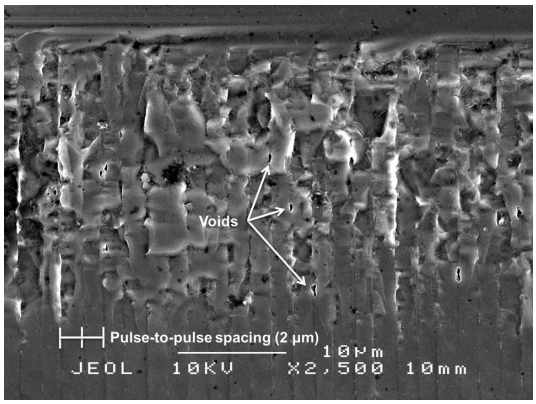

Fig. 7. Scanning electron microscopy image of a fracture plane containing pulsed-laser–induced subsurface modifications. A detail of the 2nd layer in Fig. 6 is shown.

becomes especially pronounced when a melt is formed near the focus, as it will prevent the laser radiation from reaching the focal plane. It was found that melting and fast resolidification is likely to be the damage mechanism and that the effect of diffusion is limited (see Sec. 3). This suggests that the density of absorbed energy corresponding to the modification threshold is $\approx 7.1 \times 10^3$ J/cm^3, which is the energy density that is required to heat silicon to the melting point and overcome the latent heat.

Next, measurements of the lengths of single-pulse subsurface modifications were performed, based on the sample geometry shown in Fig. 4. An example of a fracture plane containing single-pulse modifications can be found in Fig. 8. Figure 9 shows the modification length along the optical axis, as a function of the pulse energy. Again, spherical aberrations were prevented during these measurements. A quick initial rise in modification length is visible, while the growth of the modifications saturates for higher pulse energies. This saturation behavior is due to the divergence of the laser beam when moving away from the focus. The shape of the modifications may be explained by the fact that the focal volume is elongated along the optical axis (see Sec. 3).

Except for pulse energies that are very close to the modification threshold, the largest stochastic variations that were observed when measuring different single-pulse modifications inside the same sample, or when comparing multiple samples obtained using the same processing conditions, were ± 2 µm. The worst-case systematic error in the pulse energy, due to the calibration uncertainty of the power meter, is ± 5 percent. Possible sources of measurement errors that we could not quantify are: (1) the destructive sample preparation method might induce additional damage beyond the damage that was caused by the laser-material interaction and (2) damage may occur that is not detectable by optical microscopy or scanning electron microscopy.

8. Conclusions and future work

In conclusion, we have shown that laser pulses with a duration of 3.5 nanoseconds and a wavelength of 1549 nm are suitable for two-photon–induced subsurface modification of silicon, when combined with a focusing objective with a numerical aperture of 0.7. This result is consistent with predictions based on numerical simulations [20]. Additionally, it was found that the laser-induced modifications that were obtained are suitable for wafer dicing.

The reasons why the processing conditions that were considered resulted in the successful formation of subsurface modifications, contrary to previous femtosecond results, are expected

#214633 - $15.00 USD Received 23 Jun 2014; revised 14 Aug 2014; accepted 22 Aug 2014; published 3 Sep 2014

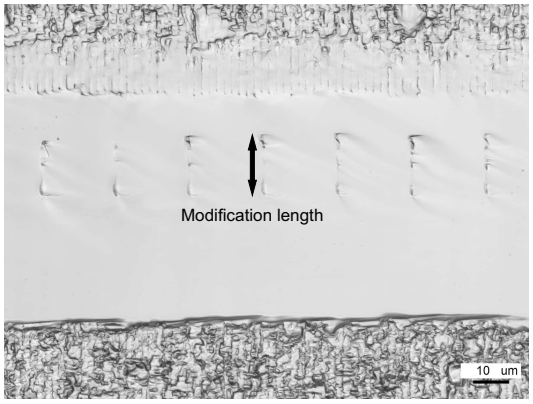

Fig. 8. Laser scanning confocal microscopy image (integrated intensity) of a fractured sample. Two layers of dense modifications (top and bottom) and a layer of separate single-pulse modifications (middle) are visible. The dense layers ensure that the sample fractures along the plane containing the modifications that are to be analyzed. On-sample pulse energy dense layers: 2 µJ, pulse energy single-pulse modifications: 0.7 µJ, transverse spacing dense layers: 2 µm, spacing single-pulse modifications: 20 µm. A 250-µm thick quartz window was used to protect the objective. The laser beam propagation direction is from top to bottom.

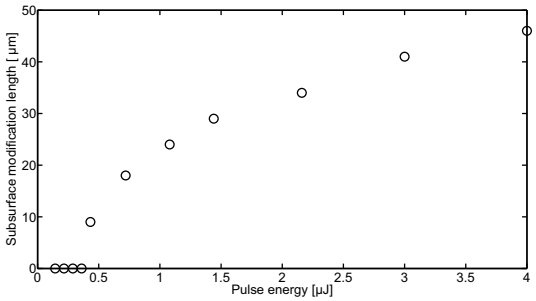

Fig. 9. Overview of experimentally obtained lengths of subsurface modifications along the optical axis, as a function of the pulse energy. Focal spot: 100 µm below the surface.

to be: (1) self-focusing due to the Kerr effect has been prevented and (2) effective multiphoton absorption only occurred in a confined volume around the focus of the beam.

Additional research is required regarding the material analysis of subsurface modifications in silicon. First, it is of interest to identify the material phases that are present in the subsurface modifications, as this can provide information about what damage mechanisms contributed to their formation. Secondly, it is important to be able to distinguish between damage that occurred during breaking and damage that is a direct result of the laser-material interaction.

Moreover, it is of interest to study the suitability of subsurface modifications in silicon for other applications than wafer dicing. The use of laser-induced subsurface modifications in silicon for optical applications has been proposed [9, 10]. A first step in this direction would be to identify the optical properties of subsurface modifications in silicon, including the changes to the refractive index. Apart from optical applications, laser modifications have shown to be capable of reducing the resistivity of polycrystalline silicon buried below dielectric material [14, 15]. It is therefore worthwhile to investigate the electrical properties of laser-induced subsurface modifications, to establish whether resistivity changes can also be induced inside (poly)silicon.

#214633 - $15.00 USD Received 23 Jun 2014; revised 14 Aug 2014; accepted 22 Aug 2014; published 3 Sep 2014

Finally, further research is recommended regarding the usability of ultra-short pulses, as these might result in different modifications compared with a nanosecond process. Since the lattice absorption of silicon is limited until a wavelength of 6 µm [37], increasing the wavelength to study the use of higher-order nonlinear absorption is an option. However, higher intensities are required to induce higher-order multiphoton absorption, while the Kerr coefficient of silicon remains fairly constant for wavelengths between 3 and 6 µm [35]. Consequently, self-focusing may prevent the successful production of subsurface modifications at long wavelengths. A solution to improve the confinement of the laser energy absorption when focusing ultra-short pulses inside silicon could be to apply temporal focusing of the beam [38, 39]. As given by the Fourier transform, ultra-short pulses have a relatively large bandwidth. By making different wavelengths follow different paths through the material towards the focus, the pulse duration outside the focus will be increased compared with the duration in the focal spot [38, 39].

Acknowledgments

This research was supported in part by Point-One.

#214633 - $15.00 USD Received 23 Jun 2014; revised 14 Aug 2014; accepted 22 Aug 2014; published 3 Sep 2014